BMC Microbiology

RESEARCH

Open Access

Seawater tides shaped mangrove sediment a bacterial community drastically distinct from supratidal land soil

Rufan Zhang[1], Lu Liu[1], Yuchen Yang[2], Shaohua Xu[2], Ziwen He[1,3], Miles E. Tracy[1,4], Suhua Shi[1,3,4*] and Zixiao Guo[1,3*]

Abstract

The intertidal zone where mangroves inhabit is unique for both plants and microbes. The periodic seawater tides have allowed only a very small portion of woody plants to shift as mangroves. However, the understanding of how seawater tides shape bacterial community in mangrove sediment is not yet comprehensive. By comparing mangrove sediment in low-tidal zones to land soil in supratidal zones, we investigated their differentiation of bacterial community in diversity, composition, interaction and functional potential, assembly mechanisms, and the underlying factors. Using 16 S ribosomal RNA (rRNA) gene sequencing, we found drastic distinctness in community composition and structure between these two types of soils. The distinctness was partially attributed to the high level of dispersal limitation in assembling processes and strongly correlated with the differences of sea tide-related edaphic conditions, including moisture, total carbon, total sulfur, salinity, and pH. The periodic inundation in mangrove sediment has also shaped a more complex and compact bacterial interaction network, and strong dispersal limitation between low-tidal and supratidal zones. With supratidal soil as the control, our findings highlight the direct influence of sea tides on bacterial community in mangrove sediments, providing support for employing microbes as early indicators of biological community change in coastal zones upon the projected sea-level rise.

Keywords Assembly process, Bacterial interaction network, Intertidal zone, Mangrove forest, Total carbon

Introduction

Mangrove forests, occurring at the interface of land and sea, provide essential protection for coasts against the tidal erosion, typhoon attack and rising sea-level [1, 2]. Mangrove wetlands are also important carbon sink with high efficiency in carbon fixation and sequestration [3]. At the intertidal zone, the unique ecosystem of mangrove forest receives material inputs from both terrestrial river and marine tide. The complex entangled aerial root system of mangrove trees traps sediment, providing substrate for plants, benthic animals, as well as soil microbes [4–6].

Microbes in the sediment play a vital ecological role in mangrove ecosystem by contributing to biogeochemical

*Correspondence:
Suhua Shi
lssssh@mail.sysu.edu.cn
Zixiao Guo
guozx8@mail.sysu.edu.cn
[1]State Key Laboratory of Biocontrol, Guangdong Key Lab of Plant Resources, School of Life Sciences, Sun Yat-Sen University, Guangzhou, Guangdong, China
[2]School of Ecology, Sun Yat-Sen University, Shenzhen, Guangdong, China
[3]Innovation Center for Evolutionary Synthetic Biology, Sun Yat-Sen University, Guangzhou, Guangdong, China
[4]Southern Marine Science and Engineering Guangdong Laboratory (Zhuhai), Zhuhai, Guangdong, China

cycles of carbon fixation, nitrogen fixation, sulfur reduction, and organic matter degradation [7]. Inundated periodically by tides, the soils (sediments) of mangrove forests are featured with fluctuations in salinity, pH, dissolved oxygen, and organic matter content [8–10], which are quite different from terrestrial lands. Hence, the prokaryotic communities in mangrove sediment have been found to have higher alpha diversity and distinct beta diversity, compared with other biomes such as freshwater river, freshwater lake, coastal zone, ocean, salt-water lake and hot spring [11].

The structure and assembly of mangrove microbial community have attracted wide attention. Multiple studies have focused on the differentiation in rhizosphere bacterial communities among different mangrove species [12–14], however such differentiation was shown to be much less than the differentiation between geographic locations, even though these locations are very close [15]. At the whole island scale, regional differentiation of bacterial functional diversity was found in Hainan Island, which was associated with both spatial variable and environmental factors such as total carbon, nitrite nitrogen and salinity [16]. Within the mangrove forests, strong variety in bacterial community composition has also been observed between the tall tree and dwarfed shrub zones [17]. Some attention has also been paid to the archaeal community in mangroves, with higher diversity found in surface sediment than in subsurface, as well as higher diversity in mangroves at low latitudes than at high latitudes [18].

Despite the hot researching interests, efforts have rarely been made to uncover the direct influence of seawater tides on bacterial diversity and community assembly in mangrove sediments. As is well-known, the varying degrees of tidal inundation has strong influence on the plant community of mangrove forests, resulting in a band-like distribution pattern of transiting from true mangrove to mangrove associate species from low-tidal to high-tidal zones. Hence, we speculated that seawater fluctuation should have also strongly shaped the sediment microbial communities in mangrove forests. Compared to the supratidal soil neighboring to mangrove forest, mangrove sediments are mainly different in edaphic conditions, such as moisture, salinity and dissolved oxygen.

Edaphic conditions, together with geographic distance, climatic conditions and plant host, are the major factors governing sediment/soil microbial community diversity and assembly [19]. In certain scenarios, edaphic conditions alone may play dominant roles. Salinity and nutrient conditions were found to have played critical role in shaping the composition, connectivity, and assembly process of prokaryotic communities of saline lakes, mangroves, ocean margins, cold seeps and open oceans, which were governed by deterministic forces [20]. Soil pH independently explained ~ 68% of the variation in composition of bacterial communities, playing as the primary determinant of bacterial diversity and community composition in natural mountain forests of eastern China [19]. Soil salinity and organic matter were also found strong determinants of archaeal community variation in saline agricultural soils, and archaea transition from stochasticity in medium salinity soils to determinism in higher salinity soils [21]. Edaphic variables have also been found to have stronger influence on abundant bacteria and fungi taxa than rare taxa in mangroves and mudflat [22].

In this study, we detected the direct influence of seawater tides on sediment microbial community, by comparing the bacterial communities of mangrove sediments to those of the supratidal zones, minimizing the cofounding factors to the greatest extent. We used 16S ribosomal RNA (rRNA) gene sequencing to explore the diversity, composition, structure, interaction network and function of the bacterial communities in mangrove sediments and supratidal soils. We hypothesize that: (1) the mangrove sediments differ significantly from supratidal soils in bacterial community; (2) the bacterial community of mangrove sediments is significantly shaped by edaphic factors such as salinity and moisture; (3) both stochastic and deterministic processes have played roles in the bacterial community assembly.

Materials and methods

Sampling sites and methods

Samples were collected from three sites in Dongzhai Harbour, Hainan Island, South China: Sanjiang (E110°37′, N19°55′), Yanfeng (E110°35′, N19°57′), and Tashi (E110°33′, N20°00′). Dongzhai harbor is a small sea bay, with a length about 12.7 km and width about 3.5 km (Figure S1). The three sites Sanjiang, Yanfeng, and Tashi, respectively, locate from inner bay, mid-bay to bay mouth. In each site, we collected mangrove sediment samples from low-tidal zone, including rhizosphere samples from roots of two true mangrove species (*Kandelia obovata* and *Aegiceras corniculatum*) and bulk samples from bare mud near mangrove trees. In parallel, supratidal soil samples were collected from areas that were not, or only rarely, inundated by seawater. Supratidal rhizosphere samples were collected from roots of two mangrove associate species (*Hibiscus tiliaceus* and *Pongamia pinnata*), and supratidal bulk samples were collected from bare soils near the trees.

For the rhizosphere samples of each species at each site, we randomly selected four to six individual trees, which were at least 5 m apart from other trees. To collect rhizosphere sediment samples, we drilled hole in the sediment to a depth of 15 cm and collected soils attached to roots.

For each tree, we drilled three holes, which are around the tree trunk from different directions, and soils from all the holes of a same tree were pooled to be used as one sample. Meanwhile, four to six bulk sediment samples were collected in each site. The bulk sediments were also collected by drilling three holes to the depth of ~15 cm, at locations at least one meter away from any trees.

Hence, a total of 94 samples were collected (Table S1), and all samples were placed in sealed polythene bags, stored on ice, and immediately transported to the laboratory for further analysis.

Measurements of edaphic conditions

Soil moisture was measured by drying at 105 °C for 16 h. The air-dried soil was mixed with water at a soil-to-water ratio of 1:5 for salinity measurement using the Mettler Toledo Seven2Go S3. Similarly, the air-dried soil was mixed with water at a soil-to-water ratio of 1:2.5 for pH assessment using the Mettler Toledo SevenEasy. The air-dried soil was grounded and sieved through a 0.15 mm mesh before used for element analysis. Total carbon (TC), total nitrogen (TN), and total sulfate (TS) concentrations were measured using a CHNOS Elemental Analyzer (vario EL cube).

DNA extraction, PCR amplification and read analysis

DNA was extracted from soil samples using the E.Z.N.A.® Soil DNA Kit (Omega Bio-tek, Norcross, GA, U.S.) following the manufacturer's instructions. The V3-V4 region of the bacterial 16S rRNA gene was amplified by PCR with the following cycling conditions: an initial denaturation at 95°C for 2 minutes, followed by 25 cycles of denaturation at 95°C for 30 seconds, annealing at 55°C for 30 seconds, extension at 72°C for 30 seconds, and a final extension at 72°C for 5 minutes. The primers used were 341F 5'-barcode-CCTACGGGNGGCWGCAG-3' and 806R 5'-GACTACHVGGGTATCTAATCC-3'. Within the primer sequence, the eight-bases barcode was used to record sample identity. The amplicons were paired-end sequenced (2 × 250) on an Illumina platform following standard protocols.

Raw reads were demultiplexed using custom Perl scripts based on barcode sequence information. The following quality control criteria were applied: (1) 10 bp sliding windows on the 250 bp raw read with an average quality score < 20 were truncated, and the truncated read was discarded if shorter than 50 bp; (2) reads with more than two nucleotide mismatches in primer regions or containing ambiguous bases were removed; (3) a read was discarded if overlapped (> 10 bps) with none of the other reads or identified as chimeric. The rarefaction analysis was used to identify a cut-off of 9000 sequences per sample to control the effect of uneven sequence distribution among samples (Figure S2).

Feature table construction and diversity analysis

QIIME2 2020.8 was used to analyze the quality-filtered sequences and identify amplicon sequence variants (ASVs) [23]. The sequences were demultiplexed and quality-filtered using the q2-demux plugin, and denoised using the q2-dada2 plugin implemented in DADA2 [24]. ASVs were generated by clustering sequences with 100% similarity. The number of sequences in each ASV cluster is inferred as the abundance, and the clusters with less than 100 sequences were excluded from downstream analyses.

Shannon index was calculated using the q2-diversity plugin [23] to evaluate alpha diversity. The indexes of weighted UniFrac and Bray-Curtis dissimilarity were calculated using the q2-diversity plugin to evaluate beta diversity. Principal coordinate analysis (PCoA) based on these beta diversity metrics was conducted using the vegan package in R. Adonis was used to test the influence of different factors (lowtidal vs. supraltidal; rhizosphere vs. bulk; and grouping by sites) on community dissimilarity. The Adonis analysis was conducted using the adonis2 function in vegan packages with 999 permutations, based on the Bray-Curtis dissimilarities. Analysis of similarity (ANOSIM) was further conducted using the *anosim* function in the q2-diversity plugin to test the significance of community structure difference between different soil types.

Community composition, biomarker discovery and prediction of function

The ASVs were taxonomically classified using the q2-feature-classifier [23] with a pre-trained Naive Bayes classifier. By referencing the representative sequences of each ASV to the SILVA SSU138 16S rRNA database [25], the ASVs were assigned to different species with confidence threshold of 70%. The method of linear discriminant analysis effect size (LEfSe) [26] was used to identify the taxa with significant abundance difference between lowtidal mangrove sediment and supratidal land soil. In this method, the Kruskal-Wallis sum-rank test was applied to evaluate the abundance differences among soil samples, followed by linear discriminant analysis (LDA) to assess the effect size of each differentially abundant taxon.

Based on these 16S rRNA gene sequences, Tax4Fun2 [27] was used to predict functional profile of the bacteria. The ASV abundance table was normalized according to the 16S copy number of each ASV. A metagenomic prediction based on KEGG orthologs (KO) was used to predict gene family counts, and these predicted counts were subsequently mapped onto KEGG pathways at level 1.

Co-occurrence network analysis

Metacommunity co-occurrence networks were constructed to assess species coexistence, using the igraph package in R [28]. To minimize the complexity introduced by the large number of rare ASVs, those ASVs with a relative abundance less than 0.01% were excluded from this analysis. An edge (interaction) was accepted if Spearman's correlation coefficients (ρ) >0.6 and false discovery rate (FDR)-corrected *p*-values < 0.01. The constructed networks were visualized using Gephi [29]. The topology of the networks was characterized by modularity, average degree, clustering coefficient, closeness centrality and betweenness centrality [30].

Factors shaping bacterial community assembling

The strength of different assembling mechanisms (dispersal limitation, homogenizing dispersal, homogeneous selection, and heterogeneous selection) was quantified using iCAMP [31].

To explore the relationship between edaphic factors and microbial community structure, we conducted a redundancy analysis (RDA) [32] using the vegan package in R. We also used the "stats" package in R to calculate Spearman's correlation, which assesses the associations between edaphic factors and the top 15 abundant phyla.

Results

Low-tidal Mangrove sediment has edaphic conditions distinct from supratidal soil

We measured the edaphic physicochemical conditions of 94 samples (Table S1 & S2). We found that salinity, moisture, total carbon and total sulfur are much higher in the low-tidal sediments than in the supratidal soils (*p*-value < 0.001, Fig. 1). pH and total nitrogen are also higher in low-tidal than in supratidal soil, but with smaller significance (*p*-value < 0.05, Fig. 1). Among the three geographic sites, these differences are stronger in Yanfeng and Sanjiang than in Tashi (Table S3). Tashi locates at the bay mouth of Dongzhai harbour, the supratidal locations there are relatively lower in altitudes and more likely inundated by seawater, compared to Sanjiang and Yanfeng.

High differentiation in community diversity

We obtained a total of 2,405,001 high-quality reads for the 94 sediment samples, with an average of 25,585 reads per sample. This depth is much higher than the average depth (9,000 reads) required to uncover the potential microbial diversity, as the rarefaction curve analysis indicated (Figure S2). As follows, we clustered these reads into 4,384 ASVs after quality control.

We used Shannon index to measure alpha diversity, revealing higher alpha diversity in the low-tidal samples

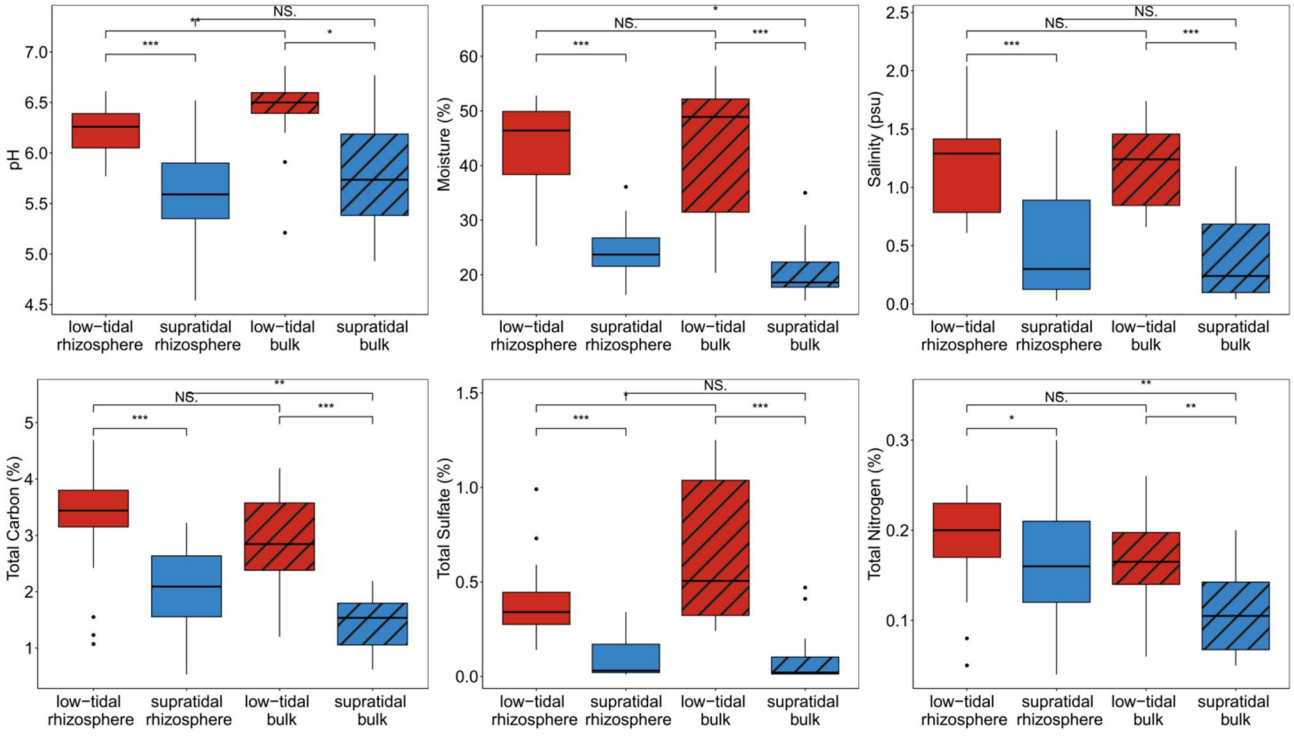

Fig. 1 Boxplots of edaphic conditions in low-tidal mangrove sediment and supratidal soil. *** means *p*-value < 0.001, ** means *p*-value < 0.01, * means *p*-value < 0.05, NS means not significant. Red box indicates low-tidal sediment and blue box indicate supratidal soil. Blank box indicate rhizosphere samples and shaded box indicates bulk samples

than in supratidal samples (Fig. 2A). This trend was consistent across most comparisons, except for bulk samples from Yanfeng and rhizosphere samples from Tashi. Notably, the alpha diversity is statistically significant higher (p-value < 0.05) in rhizosphere samples of Yanfeng and Sanjiang (Fig. 2A). The comparisons between rhizosphere and bulk samples in same tidal zones show higher alpha diversity in rhizosphere samples (Fig. 2A).

Microbial community beta diversity of the 94 samples was analyzed using Principal coordinate analysis (PCoA), based on the weighted UniFrac distances. We revealed that the most pronounced differentiation occurs between low-tidal (*A. corniculatum* and *K. obovata*) and supratidal (*H. tiliaceus* and *P. pinnata*) rhizosphere samples along the first principal axis (PCoA 1), which explained 50.42% of the total variation. Lesser but also marked difference was observed along the PCoA1 between low-tidal and supratidal bulk samples (Fig. 2B). Along the second principal axis (PCoA 2), which explained 15.81% of the total variation, the rhizosphere samples diverged from bulk samples. We used the Anonis to test the significance of different grouping methods, revealing the most significant grouping by lowtidal vs. supratidal ($R^2 = 0.18$) (Fig. 2B, Table S4).

The ANOSIM analysis based on Bray-Curtis dissimilarity uncovered a pattern consistent with the PCoA analysis and Adonis test (Fig. 2C-F). In all four comparisons, the variation between groups are higher than within each group. The most significant dissimilarity was observed between low-tidal and supratidal rhizosphere ($R = 0.910$, Fig. 2E) and the difference between low-tidal and supratidal bulk was also substantial ($R = 0.418$, Fig. 2F). We also observed significant dissimilarity between rhizosphere

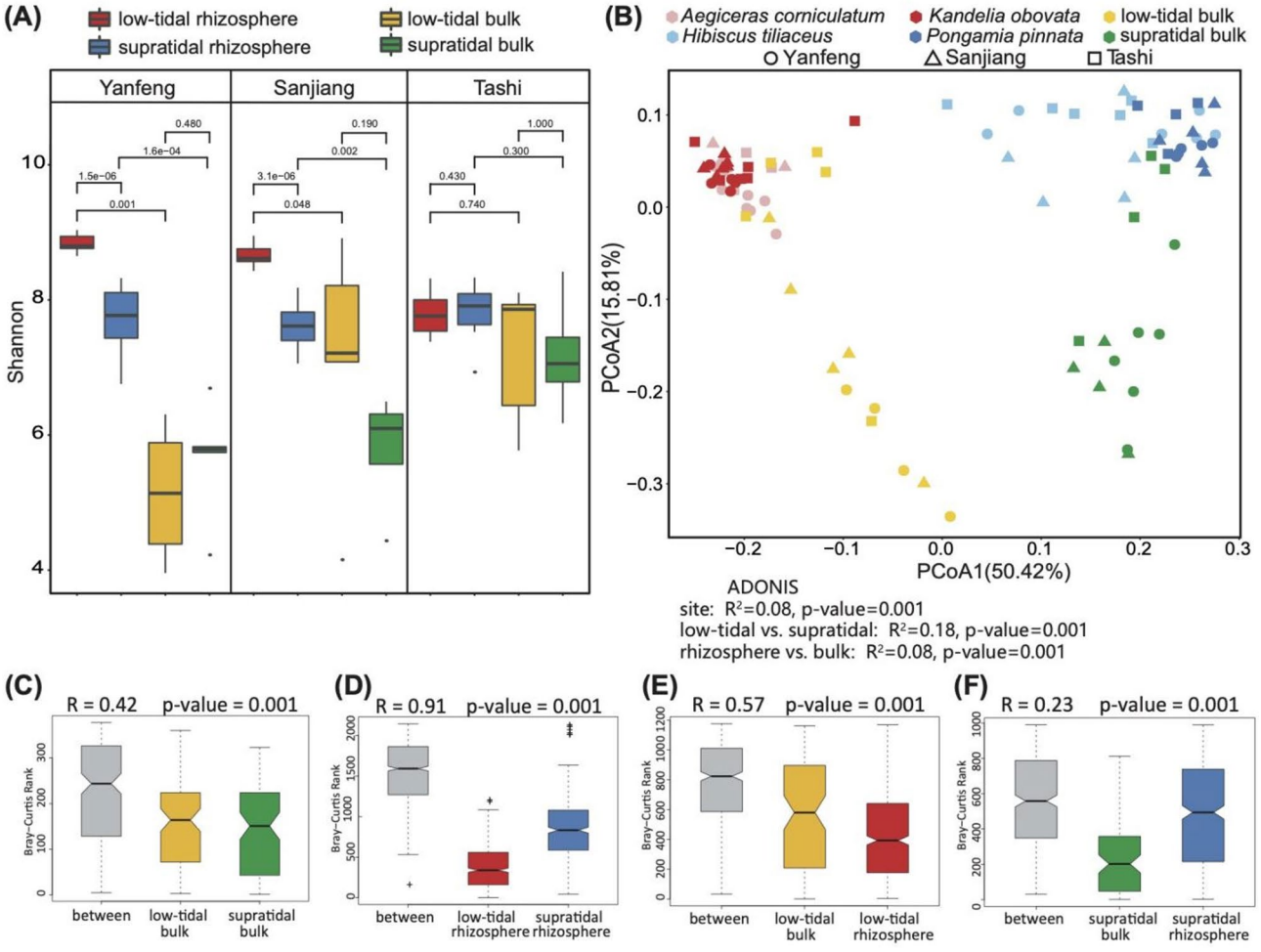

Fig. 2 Diversity of bacterial community in low-tidal mangrove sediment and supratidal soil. **A** Boxplots of Shannon index in different soils. The numbers on lines indicate p-values from Wilcoxon test. **B** PCoA plots based on weighted Unifrac distance. Point shapes indicate sampling location and point colors indicate soil types. **C**-**F** Boxplots of ANOSIM based on Bray-Curtis distance. "Between" denotes the rank of Bray-Curtis distances across different groups. Red, yellow, blue, and green boxes represent the rank of Bray-Curtis distances within the low-tidal rhizosphere, low-tidal bulk, supratidal rhizosphere, and supratidal bulk groups, respectively. From left to right are the comparisons of low-tidal bulk vs. supratidal bulk (**C**), low-tidal rhizosphere vs. supratidal rhizosphere (**D**), low-tidal bulk vs. low-tidal rhizosphere (**E**), and supratidal bulk vs. supratidal rhizosphere (**F**)

and bulk samples in both low-tidal ($R = 0.569$) and supratidal ($R = 0.231$) zones (Fig. 2C&D).

Clear differentiation in microbial community composition

A total of 41 phyla were identified across all samples. On the phylum level, Proteobacteria is the most abundant in almost all samples, accounting for ~25% of the total sequences per sample (Fig. 3). The less but also abundant phyla include Actinobacteriota, Acidobacteriota, Chloroflexi, Desulfobacterota, Bacteroidota, and Verrucomicrobiota, but their relative abundances differ among different groups of samples (Fig. 3). Firstly, Choloflexi and Desulfobacteriota occur with high frequency in the low-tidal (both rhizosphere and bulk) samples, but with lower frequency in supratidal (both rhizosphre and bulk) samples (Fig. 3, Table S5). Particularly, Bacteroidota occurs with high frequency specifically only in low-tidal rhizosphere samples (Fig. 3). In contrast, Actinobacteriota, Acidobacteriota, and Verrucomicrobiota occur with high frequency in supratidal samples but with lower frequency in low-tidal samples (excepting Actinobacteriota in low-tidal bulk samples of Yanfeng, Fig. 3).

We used the LEfSe method, which was based on the 16S-based phylometagenomic dataset, to identify the bacterial taxa indicative of the low-tidal or supratidal soils. We found similar distributions of low-tidal taxa and supratidal taxa on the phylogenetic trees constructed for the rhizosphere or bulk samples. The difference between low-tidal and supratidal taxa is clear on the taxonomic hierarchy of Phylum or Class. The phyla, including Desulfobacterota, Campilobacterota, Bacteroidota, MBNT15, and Nitrospitota are exclusively enriched in low-tidal soils (Fig. 4). In contrast, the phyla Verrucomicrobiota and Palnctomycetota are exclusively enriched in supratidal soils. Meanwhile, within the phyla Actinobacteriota, Acidobacteriota and Proteobacteria, different classes are enriched in either low-tidal or supratidal soils (Fig. 4). Particularly, within the phylum Proteobacteria, the class Alphaproteobacteria is enriched in supratidal soils, while the class Gammaproteobacteria is enriched in low-tidal soils (Fig. 4).

Functional profile of the microbial communities

We further used Tax4Fun2 to explore the functional profiles of the bacteria in metabolism pathways from different soil types (low-tidal rhizosphere, supratidal rhizosphere, low-tidal bulk and supratidal bulk) (Fig. 5). In most of the 62 metabolism-related pathways (level 1), these four sediment types have comparable percentages (Fig. 5). With 0.005 as the cutoff, 11 pathways were identified as enriched, including sulfur metabolism, pyruvate metabolism, propanoate metabolism, oxidative phosphorylation, methane metabolism, glyoxylate and dicarboxylate metabolism, glycolysis/gluconeogenesis, carbon fixation pathways in prokaryotes, butanoate metabolism, benzoate degradation, as well as amino sugar and nucleotide sugar metabolism (Fig. 5). Particularly, among these enriched pathways, significantly higher percentages in low-tidal than in supratidal soils (p-value < 0.05, Wilcoxon test) were observed in oxidative phosphorylation, methane metabolism, carbon fixation, and glyoxylate and dicarboxylate metabolism (Fig. 5).

Metacommunity co-occurrence network reveals modularization between low-tidal and supratidal soils

We constructed the bacterial co-occurrence networks for low-tidal vs. supratidal soils, with either rhizosphere or bulk samples. At the entire network scale, the two networks are comparable in statistics of node number (770 vs. 639), edge number (21795 vs. 17285), average clustering coefficient (0.637 vs. 0.532), average path length (2.683 vs. 2.661), average degree (56.61 vs. 54.10) and

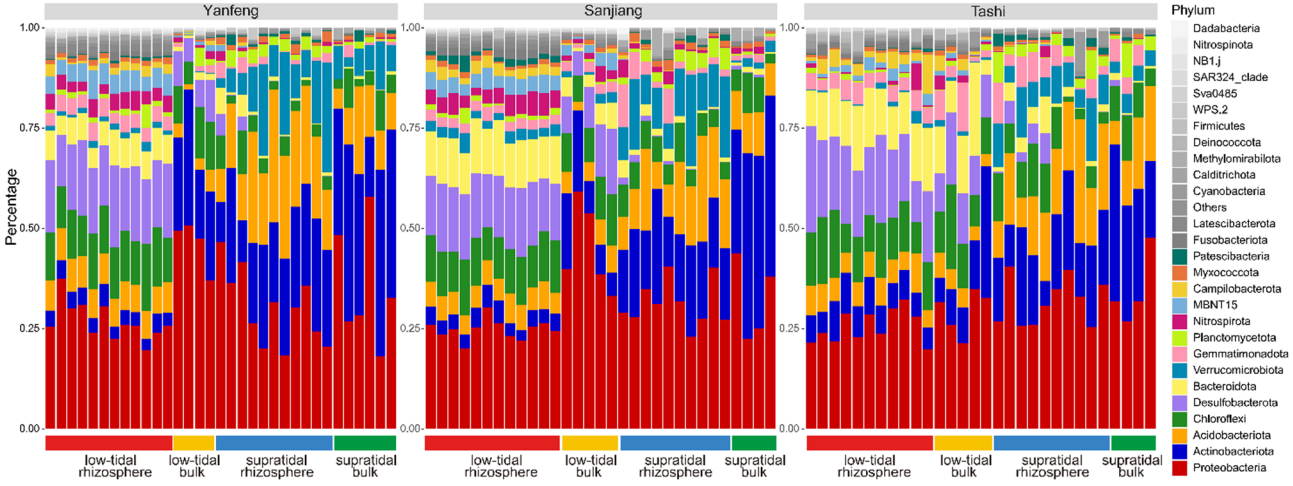

Fig. 3 Abundance of bacteria from different phyla in low-tidal mangrove sediment and supratidal soil. The top 14 abundant phyla are showed in different colors and other phyla with lower abundance are showed by a grey gradient

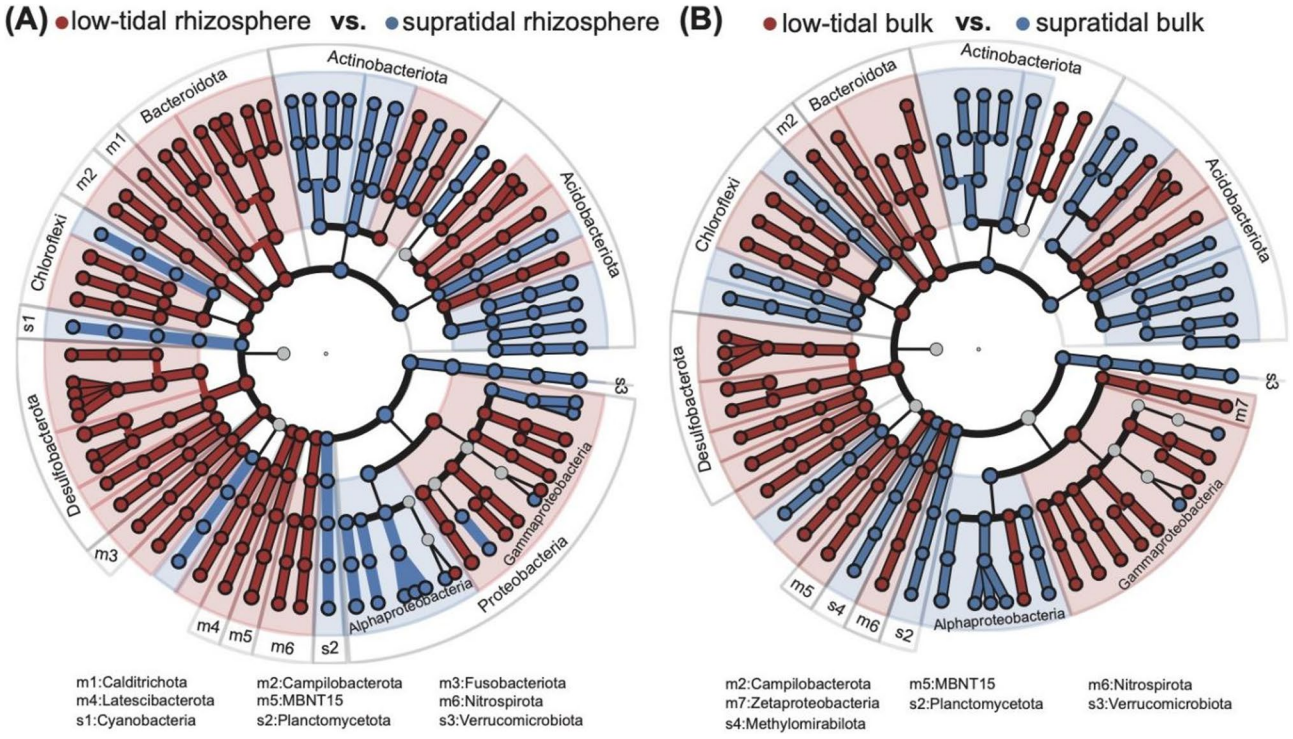

Fig. 4 Key taxa contributed for compositional and functional difference between low-tidal sediment and supratidal soils. Phylogenetic view of the linear discriminant analysis effective size (LEfSe) for rhizosphere samples (**A**) and bulk samples (**B**). From inner to outer, the tracks show nodes on the taxonomic levels of phylum, class, order, family, and genus, respectively. Each node represents a taxon. The red or blue background indicates significant higher abundance in low-tidal sediment or supratidal soils, and grey background indicates no significant difference

modularity (0.603 vs. 0.585) (Figs. 6 and 7). Interestingly, both networks tend to be subdivided into two modules, with one module mainly consists of low-tidal nodes and the other module mainly consists of supratidal nodes (Figs. 6A and 7A). Extensive positive interactions occur between nodes from the same module and extensive negative interactions occur between nodes from different modules (Figs. 6A and 7A). Such a pattern was observed in both the rhizosphere and bulk networks, and the subdivision is more prominent in the bulk than in the rhizosphere network, indicated by the smaller number of average clustering coefficient, lower proportions of negative interaction (80.17% vs. 88.56%) and higher proportion of positive interaction (19.83% vs. 11.44%).

In both of the rhizosphere and bulk networks, the low-tidal module has more nodes and intra-module interactions than the supratidal module (Figs. 6A and 7A). Consistently, the statistics of degree (Figs. 6B and 7B) and closeness centrality (Figs. 6C and 7C), which are used to capture the features of these networks, are significantly higher (p-value < 0.01) in the low-tidal than in the supratidal module, suggesting that the low-tidal modules are more intensively connected and compact. The low-tidal nodes have 68 and 76 edges on average, while the supratidal nodes have 46 and 36 edges, in the rhizosphere and bulk networks, respectively. The betweenness centrality is not significantly different between the two modules (Figs. 6D and 7D). The top 5% nodes with high degree were inferred as key nodes in each network. We reveal most of these key nodes are low-tidal taxa and belong to the phyla Acidobacteriota, Chloroflexi, Desulfobacterota, and Proteobacteria (Figs. 6E and 7E).

We conducted the same analysis for rhizosphere vs. bulk samples with either low-tidal or supratidal samples. Notably, the low-tidal network has more nodes (619 vs. 394), more edges (3097 vs. 1808) but lower modularity (0.447 vs. 0.715) than the supratidal network (Figure S3). Comparing rhizosphere with bulk nodes, we found higher levels of degree and closeness centrality in both networks (Figure S4).

Edaphic factors contribute significantly to shape bacterial community

Consistent with the PCoA analysis showed above, the RDA analysis identified remarkable bacterial diversity differentiation between low-tidal and supratidal soils mainly along the RDA1 (26.63%) in both rhizosphere and bulk samples (Fig. 8A). In comparison, much lower but still notable differentiation was observed between the rhizosphere and bulk soils mainly along the RDA2 (5.71%) in both low-tidal and supratidal zones (Fig. 8A). In this analysis, we can further identify the edaphic factors that

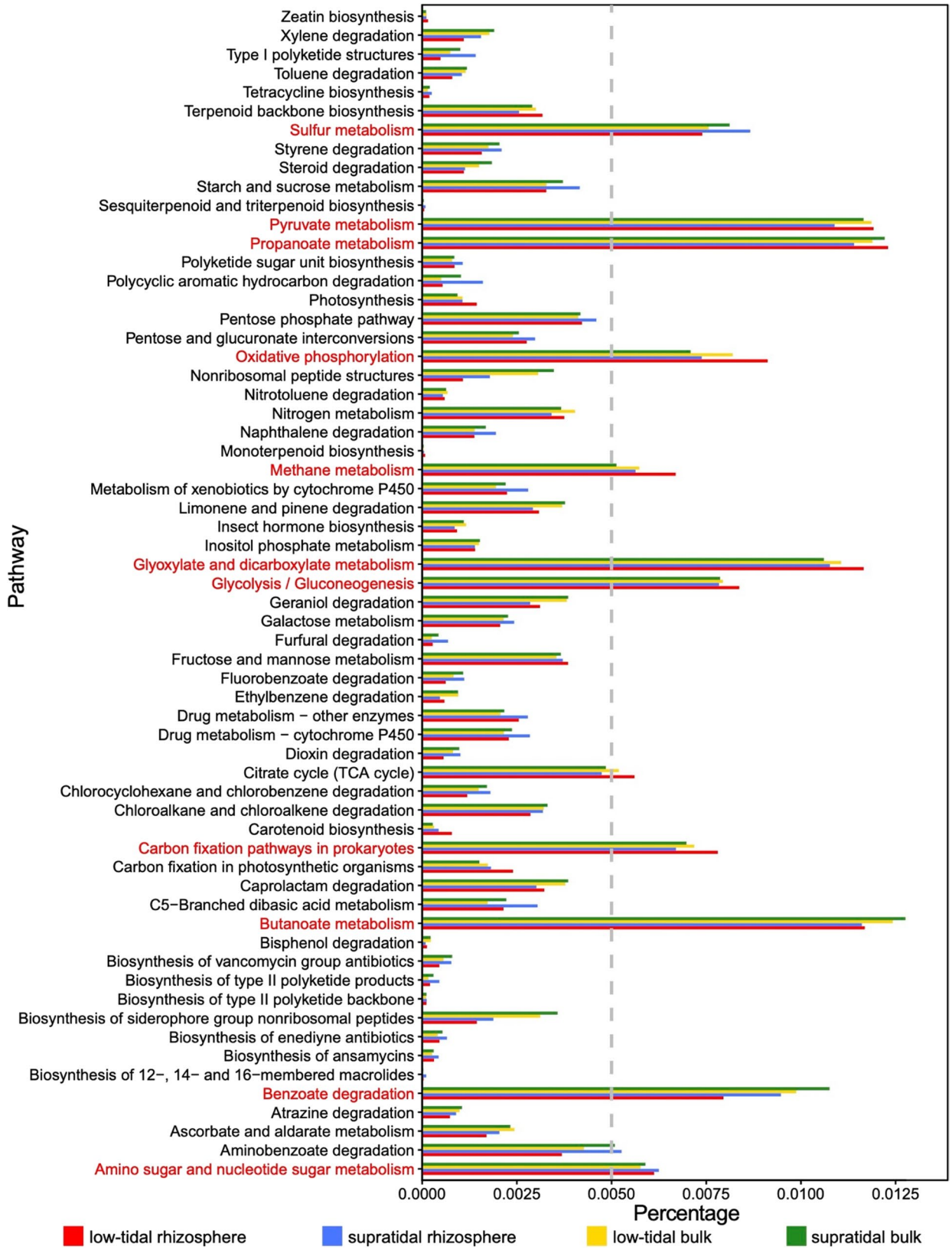

Fig. 5 Barplots showing the functional profiles. The bars are average abundances (percentages) of different metabolism pathways. Pathways in red are the top abundant ones that all the four samples have percentages above 0.005

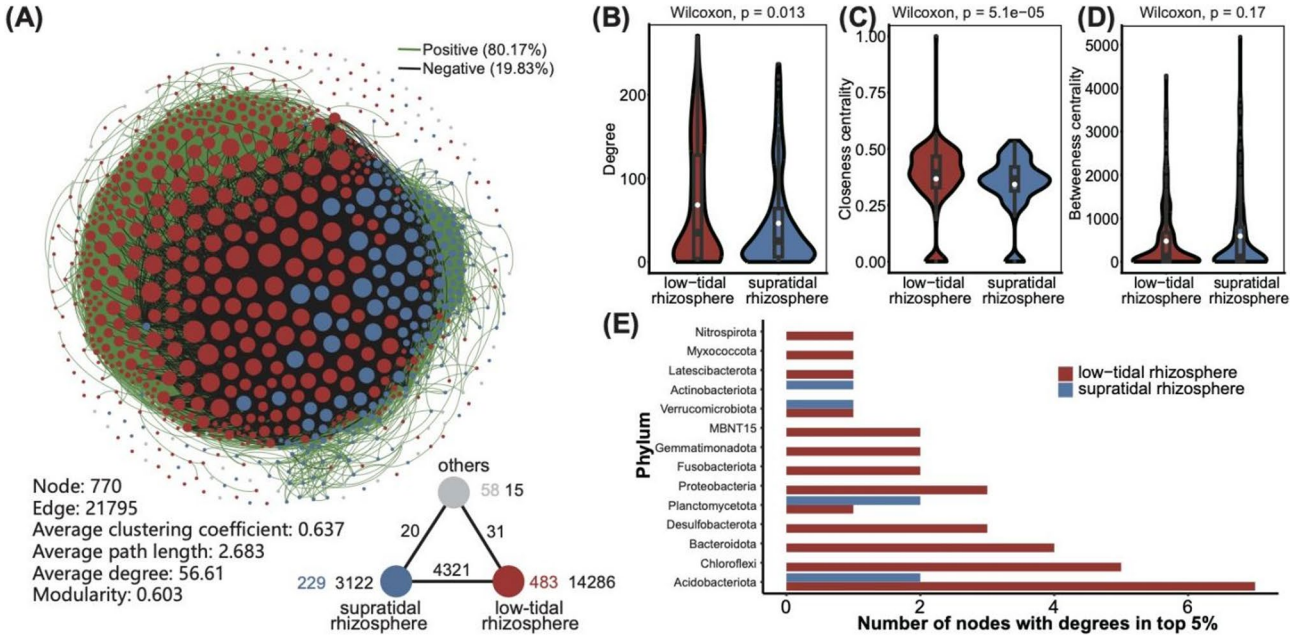

Fig. 6 Metacommunity co-occurrence network of low-tidal sediment and supratidal soil rhizosphere samples. **A** In the networks, positive and negative interactions are depicted in green and dark gray edges, respectively. The nodes correspond to ASVs, with node size proportional to degree. In the bottom of each panel, we used a triangular sketch to summarize the number of nodes and edges. In the sketch, the colored numbers indicate module-specific node counts, the dark numbers nearby indicate intra-module connections, and the numbers adjected to lines indicate inter-module interactions. **B** Violin plots showing the distribution of degree. **C** Violin plots showing the distribution of closeness centrality. **D** violin plot showing the distribution of between centrality. **E** Barplots showing key nodes with top 5% degrees

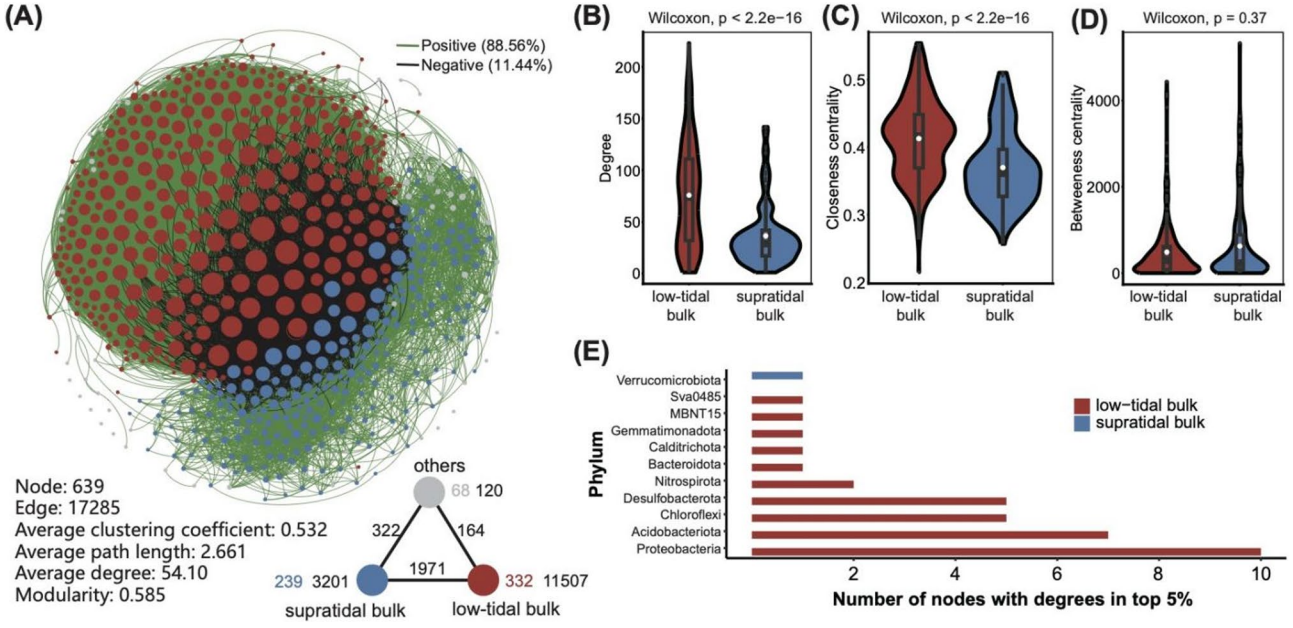

Fig. 7 Metacommunity co-occurrence network of low-tidal sediment and supratidal soil bulk samples. **A** In the networks, positive and negative interactions are depicted in green and dark gray edges, respectively. The nodes correspond to ASVs, with node size proportional to degree. In the bottom of each panel, we used a triangular sketch to summarize the number of nodes and edges. In the sketch, the colored numbers indicate module-specific node counts, the dark numbers nearby indicate intra-module connections, and the numbers adjected to lines indicate inter-module interactions. **B** Violin plots showing the distribution of degree. **C** Violin plots showing the distribution of closeness centrality. **D** violin plot showing the distribution of between centrality. **E** Barplots showing key nodes with top 5% degrees

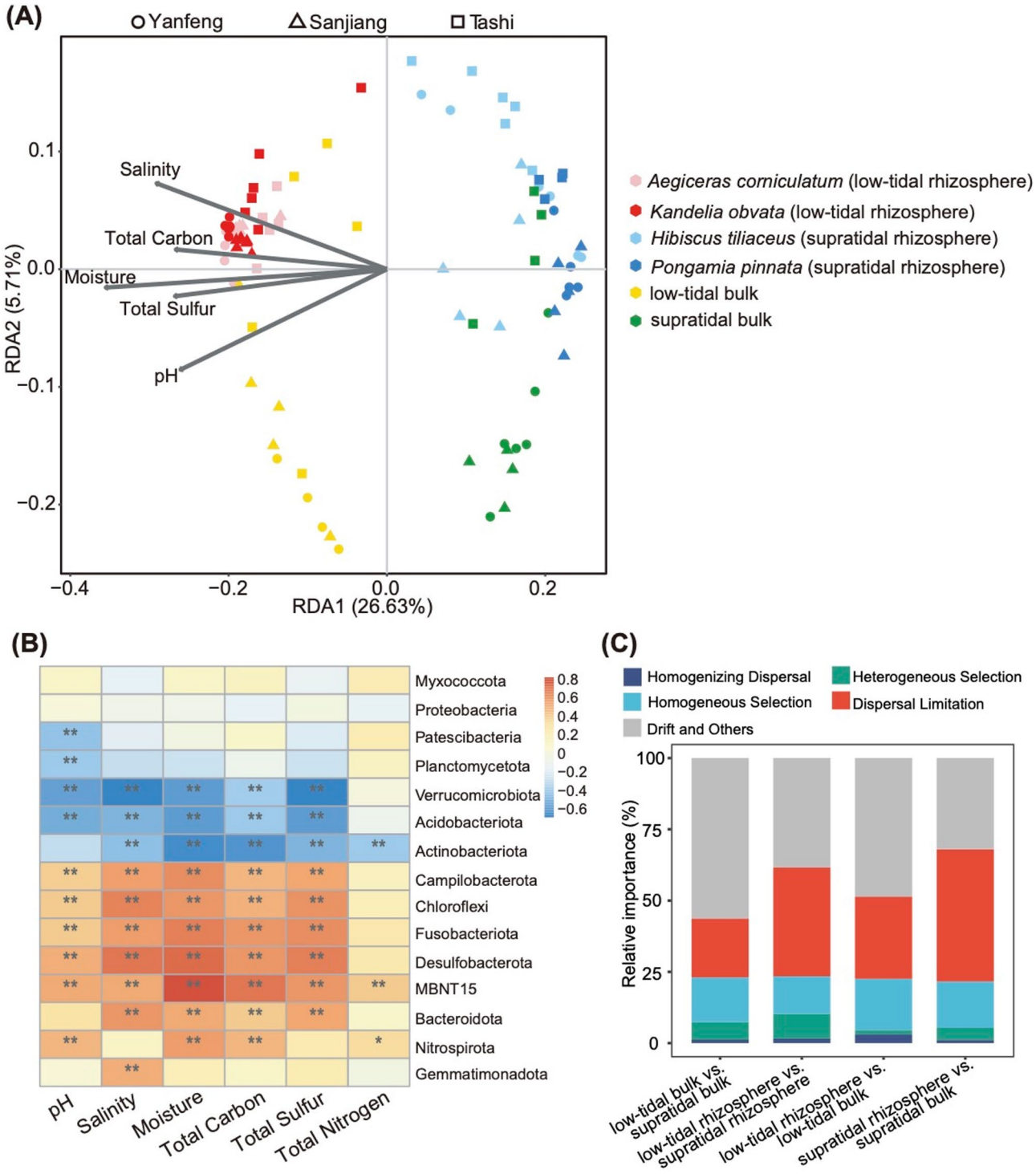

Fig. 8 Edaphic factors and assembly process contributed to bacterial community differentiation between low-tidal sediment and supratidal soil. **A** RDA biplot showing the covarying edaphic factors with the microbial community structure. Arrows indicate the significant factors (p-value < 0.05). Point shapes indicate sampling location, point color indicates soil source. **B** Heatmap of correlation between edaphic factors and relative abundances of top 15 phyla. ** means p-value < 0.01, * means p-value < 0.05. **C** Assembly mechanisms underlying bacterial communities of low-tidal mangrove sediment and supratidal soil. Proportions of different assembly mechanisms that were computed for the different combinations of sediment types

contributed to these differentiations. We found that moisture, total carbon and total sulfur (p-values < 0.001) contributed significantly to the differentiation between low-tidal and supratidal soils. Meanwhile, salinity and pH also contributed to the differentiation between low-tidal and supratidal soils, as well as between rhizosphere and bulk soils.

We used the Spearman's correlation analysis to identify the edaphic factors that are correlated with the top 15 abundant phyla (Fig. 8B). The relative abundances of Desulfobacterota, Chloroflexi, Campilobacteriota, Fusobacteriota and MBNT15 are positively correlated with moisture, total carbon, total sulfur, pH, and salinity. Bacteroidota is also positively correlated with four of these factors (excepting pH). In contrast, Verrucomicrobiota and Acidobacteriota are negatively correlated with these five factors (Fig. 8B) and Actonobacteriota is negatively correlated with four of these five factors (excepting pH).

Assembly mechanisms underlying bacterial community

We used iCAMP to infer the proportions of different forces (dispersal limitation, homogenizing dispersal, homogeneous selection, heterogeneous selection and drift and others) in assembling the bacterial communities. Notably, drift and others assigned by the iCAMP method is the unexplainable factors in assembly mechanisms [33], thus it is not taken into consideration here. Among the remaining four mechanisms, dispersal limitation and homogeneous selection take high proportions in all computations (Fig. 8C). The relative contributions of these processes are generally consistent among the three sites (Yanfeng, Sanjiang, and Tashi) (Figure S4). Notably, in assembling low-tidal and supratidal communities (low-tidal bulk vs. supratidal bulk; low-tidal rhizosphere vs. supratidal rhizosphere), heterogeneous selection shows higher proportions while homogeneous selection shows lower proportions than the two comparisons between rhizosphere and bulk samples (Fig. 8C). On the other hand, when comparing rhizosphere and bulk samples, we found higher proportions of dispersal limitation in supratidal zones than in low-tidal zones.

Discussion

Microbial diversity affected by seawater inundation

We provide compelling evidences that the bacterial communities in mangrove sediment (low-tidal) soil are significantly different from those in the closely neighboring supratidal land soil. The mangrove sediment soil, both in rhizosphere and bulk samples, shows higher alpha diversity. Previous studies have also reported high bacterial diversity in the sediments of mangrove forests located in southeastern China [11, 18, 34], southern China [15, 35] and Kenya [13].The PCoA analysis indicated half of the variation is partitioned between low-tidal and supratidal, much higher than the proportion between rhizosphere and bulk. As all the three sampling sites locate in the same bay, climate conditions are the same, hence edaphic factors may have major contribution to the bacterial difference between low-tidal and supratidal soil.

Our RDA analysis showed moisture, total carbon and total sulfur have made the most contribution to this bacterial differentiation between mangrove sediment and supratidal soil. Meanwhile, salinity and pH are also relevant. Mangrove sediment is periodically inundated by sea tides, while supratidal lands, where mangrove associate species occur, are rarely inundated. Hence, the difference in moisture and salinity is obvious. The reduced moisture in supratidal soil may constrain microbial growth, biomass, and diversity, due to reduced material exchange and biochemical reactions [36–39]. In contrast, the high moisture in mangrove sediments may indirectly influence rhizosphere microbial diversity through plant-microbe interactions [40–42]. Previous studies have showed that the frequency of rewetting and drying significantly affects diversity, relative abundance, and phylogenetic structure of microbial communities [43–45]. The more fluctuated low-tidal zones are more likely to shape numerous micro niches, which support a more diverse microbial community.

Within the low-tidal or supratidal zone, rhizosphere soil commonly has higher bacterial diversity (Fig. 2A). Plant roots release compounds like amino acids, lipids, and vitamins that stimulate microbial activity and increase rhizosphere diversity [46–49]. The interaction between plant roots and microbial communities may also alter the microenvironment within the rhizosphere [48–50]. We observed lower pH, higher total carbon, higher total sulfur and higher total nitrogen in rhizosphere than in bulk soil. This pattern is observed in both low-tidal and supratidal samples, though not all the comparisons is statistically significant.

Enriched bacteria with important ecological function in mangrove sediment

Our study revealed that Proteobacteria, Chloroflexi, Desulfobacterota, Actinobacteriota, Acidobacteriota, and Bacteroidota are the most abundant taxa in both low-tidal and supratidal soils, which is roughly consistent with previous studies in China [11, 15, 51]. The most abundant bacterira could be various among different regions, particularly at larger geographic scale. For examples, previous studies found enrichment of Firmicutes in mangrove sediments of India [52] and Brazil [53]. Parvarchaeota and Cyanobacteria were found to have substantial abundance in mangrove forests from Beilun Estuary, China [54]. Notably, Proteobacteria, Chloroflexi, and Desulfobacteriota have been proposed as core microbiota

of mangrove ecosystem by comparing of samples at the global scale [55].

Our study underlined that distinct taxa are enriched in the mangrove sediment and supratidal land soils. In the low-tidal mangrove sediment, Desulfobacterota, Chloroflexi, and Bacteroidota are highly abundant, while Actinobacteriota and Acitinobacteriota are more abundant in supratidal soil. Such distinctness in composition is consistent with the estimation of high proportions of dispersal limitation in assembling these bacterial communities. Interestingly, higher levels of dispersal limitation are observed in rhizosphere than in bulk communities (Fig. 8C), probably due to that rhizosphere sediments in low-tidal and supratidal zones are spatially isolated while bulk soils are not. Similarly, tidal currents in the low-tidal zone might have facilitate dispersal of bacteria, resulting in lower level of dispersal limitation in low-tidal zones than in supratidal zones (Fig. 8C).

The enrichment of the core bacteria in mangrove sediment reflects their adaptability to the unique soil environment. The most predominant Gammaproteobacteria are involved in carbon, nitrogen, and sulfur cycles [56, 57]. Deltaproteobacteria are known greatly represented in methane transformations, Alphaproteobacteria, Betaproteobacteria and Deltaproteobacteria played key roles in nitrogen transformations [53].

Desulfobacterota consists of many sulfate-reducing bacteria, these bacteria thrive in anoxic environment and play a role in carbon fixation through the acetyl-CoA pathway, efficiently synthesizing acetic acid in anaerobic conditions [58–60]. The anoxic conditions in mangrove sediment provide a suitable environment for these bacteria.

Chloroflexi grow photoheterotrophically in light-limited and hypoxic conditions, contributing to carbon fixation through the 3-hydroxypropionate pathway [61, 62]. Our data show significant correlation between Chloroflexi abundance and total carbon (Fig. 6B). The abundant Chloroflexi bacteria in the low-tidal mangrove sediment are likely contribute much to the carbon cycling in mangroves, thus playing an important role in carbon sequestration within mangrove ecosystems.

In contrast, the most abundant taxa in supratidal land soils are Actinobacteriota, Acidobacteriota, and Verrucomicrobiota. Known for their resistance to drought stress, the enrichment of Actinobacteriota and Verrucomicrobiota in supratidal soil is not beyond expectation [63–66].

Modularized microbial networks imply niche filtering by seawater tides

We observed that the low-tidal and supratidal nodes are distinctly corresponding to two distinct modules in the co-occurrence network. The modularity between soil types (habitats) indicates stong environmental filtering of microbials. Previous studies have also shown environmentally-driven modules due to water depth [67] or soil properties [68]. The intensive negative interaction between modules may imply co-exclusion mechanisms, such as direct competition, toxin production, environmental modification, and differential adaptation [69, 70]. In contrast, the interactions within each module are mostly positive, implying collaboration or niche sharing.

The two modules show different topological profiles. Compared to the supratidal module, the low-tidal one has more nodes, more edges and higher number of node degrees, i.e. the low-tidal microbial community tend to be a more complex network with extensive interactions. The higher number of nodes is consistent with the higher alpha diversity there. This difference is likely attributed to the rhythmical tides in low-tidal zones. First, the tides exchange seawater flow periodically between mangrove forest and outside open sea, promoting bacterial migration. Second, the environmental conditions in low-tidal mangrove sediments are much more fluctuated and dynamic, which may promote bacterial interaction.

However, as the May-Wigner theory predicted, a large and highly-connected network is intrinsically unstable [71]. Hence, it is unclear how mangrove sediment maintains an unstable bacterial network in the unstable environment. We observed that the low-tidal module has also higher value of closeness centrality, implying a denser and more compact network. Probably, compared to the random network proposed in the May-Wigner theory, microbial networks are natural networks with structural properties such as interaction strength, modularity, and nestedness. A likely explanation is that weaker interaction strengths may drive stability in large ecological networks [72]. Stronger interactions have been found to decrease the stability of microbial communities [73]. Despite higher average degree in the low-tidal bacterial communities, species interactions in the low-tidal sediments are likely weaker due to higher nutrient availability.

Conclusions and prospects

This study demonstrated the pivotal role of seawater tides in shaping mangrove sediment bacterial communities, influencing their diversity, composition, structure, and interaction networks, and thereby highlighting the distinct differences from soil bacterial communities in supratidal coastal lands. Considering the projected global rise in sea levels, mangrove forests worldwide, together with adjacent low-lying coastal areas, are expected to be increasingly affected by tidal dynamics in the near future. It should be noted, however, that the present investigation was restricted to a single bay on Hainan Island, China. Broader comparative analyses across multiple mangrove ecosystems are therefore required to determine whether the mechanisms identified here are consistent at larger

spatial scales. Given the central role of bacterial communities in biogeochemical cycling and soil development, these findings provide critical insights to inform strategies for mangrove conservation and coastal protection, while offering scientific evidence to predict ecosystem responses to sea-level rise and to employ microbes as early indicators of environmental change.

Supplementary Information

The online version contains supplementary material available at https://doi.org/10.1186/s12866-025-04486-3.

Supplementary Material 1.

Authors' contributions

Guo Z. and Shi S. conceived and supervised the study. Zhang R. and Liu L. collected samples and sequence data. Zhang R., Liu L., Yang Y., Xu S., He Z., and Tracy M. analyzed the data. Zhang R. and Guo Z. wrote the draft manuscript and revised the manuscript. Tracy M. helped in English language editing. All authors have read and approved the final manuscript.

Funding

This work is funded by National Natural Science Foundation of China (No. 42276159, No. 42476134 and No. 32330005) and Guangdong Natural Science Foundation (No. 2023A1515012406).

Data availability

The raw sequence data reported in this paper are available in the Genome Sequence Archive in National Genomics Data Center (accession number GSA: CRA024176; project number PRJCA037764), which are publicly accessible at [https://ngdc.cncb.ac.cn/gsa/browse/CRA024176](https:/ngdc.cncb.ac.cn/gsa/browse/CRA024176) (accessed on Oct. 11. 2025).

Declarations

Ethics approval and consent to participate

Not applicable.

Consent for publication

Not applicable.

Competing interests

The authors declare no competing interests.

Received: 31 July 2025 / Accepted: 15 October 2025
Published online: 14 November 2025

References

1. De Lacerda LD. Mangrove ecosystems: function and management. Springer Science & Business Media; 2002.
2. Temmerman S, Meire P, Bouma TJ, Herman PMJ, Ysebaert T, De Vriend HJ. Ecosystem-based coastal defence in the face of global change. Nature. 2013;504:79–83. https://doi.org/10.1038/nature12859.
3. Wang F, Sanders CJ, Santos IR, Tang J, Schuerch M, Kirwan ML, et al. Global blue carbon accumulation in tidal wetlands increases with climate change. Natl Sci Rev. 2021;8:nwaa296. https://doi.org/10.1093/nsr/nwaa296.
4. Azam F, Malfatti F. Microbial structuring of marine ecosystems. Nat Rev Microbiol. 2007;5(10):782–91. https://doi.org/10.1038/nrmicro1747.
5. Kathiresan K, Bingham BL. Biology of Mangroves and Mangrove ecosystems. Adv Mar Biol. 2001;40:81–251. https://doi.org/10.1016/S0065-2881(01)40003-4.
6. Tomlinson PB. The botany of mangroves. Cambridge University Press; 2016.
7. Helfer V, Hassenrück C. Chapter 6 - Microbial communities in Mangrove sediments. In: Sidik F, Friess DA, editors. Dynamic sedimentary environments of Mangrove Coasts. Elsevier; 2021. pp. 141–75. https://doi.org/10.1016/B978-0-12-816437-2.00003-3.
8. Castine SA, Bourne DG, Trott LA, McKinnon DA. Sediment microbial community analysis: Establishing impacts of aquaculture on a tropical Mangrove ecosystem. Aquaculture. 2009;297:91–8. https://doi.org/10.1016/j.aquaculture.2009.09.013.
9. Chen Q, Zhao Q, Li J, Jian S, Ren H. Mangrove succession enriches the sediment microbial community in South China. Sci Rep. 2016;6:27468. https://doi.org/10.1038/srep27468.
10. Zhuang W, Yu X, Hu R, Luo Z, Liu X, Zheng X, et al. Diversity, function and assembly of Mangrove root-associated microbial communities at a continuous fine-scale. NPJ Biofilms Microbiomes. 2020;6:52. https://doi.org/10.1038/s41522-020-00164-6.
11. Zhang C-J, Pan J, Duan C-H, Wang Y-M, Liu Y, Sun J, et al. Prokaryotic diversity in mangrove sediments across southeastern China fundamentally differs from that in other biomes. mSystems. 2019;4e00442–19 . https://doi.org/10.1128/msystems.00442-19.
12. Zhang Y, Yang Q, Ling J, Van Nostrand JD, Shi Z, Zhou J, et al. Diversity and structure of diazotrophic communities in Mangrove rhizosphere, revealed by high-throughput sequencing. Front Microbiol. 2017. https://doi.org/10.3389/fmicb.2017.02032. 8 OCT.
13. Muwawa EM, Obieze CC, Makonde HM, Jefwa JM, Kahindi JHP, Khasa DP. 16S rRNA gene amplicon-based metagenomic analysis of bacterial communities in the rhizospheres of selected mangrove species from Mida Creek and Gazi Bay, Kenya. PLoS One. 2021;16(3). https://doi.org/10.1371/journal.pone.0248485.
14. Sui J, He X, Yi G, Zhou L, Liu S, Chen Q, et al. Diversity and structure of the root-associated bacterial microbiomes of four Mangrove tree species, revealed by high-throughput sequencing. PeerJ. 2023;11. https://doi.org/10.7717/peerj.16156.
15. Liu L, Wang N, Liu M, Guo Z, Shi S. Assembly processes underlying bacterial community differentiation among geographically close Mangrove forests. mLife. 2023;2:73–88. https://doi.org/10.1002/mlf2.12060.
16. Wang H, Tian T, Gong Y, Ma S, Altaf MM, Wu H, et al. Both environmental and Spatial variables affect bacterial functional diversity in Mangrove sediments at an Island scale. Sci Total Environ. 2021;753. https://doi.org/10.1016/j.scitotenv.2020.142054.
17. Thomson T, Fusi M, Bennett-Smith MF, Prinz N, Aylagas E, Carvalho S, et al. Contrasting effects of local environmental and biogeographic factors on the composition and structure of bacterial communities in arid monospecific mangrove soils. 2022;10(1):e00903–21 .
18. Zhang Z-F, Pan J, Pan Y-P, Li M, Biogeography. Assembly Patterns, driving Factors, and interactions of archaeal community in Mangrove sediments. mSystems. 2021;6. https://doi.org/10.1128/msystems.01381-20.
19. Ni Y, Yang T, Ma Y, Zhang K, Soltis PS, Soltis DE, et al. Soil pH determines bacterial distribution and assembly processes in natural mountain forests of Eastern China. Glob Ecol Biogeogr. 2021;30:2164–77. https://doi.org/10.1111/geb.13373.
20. Zhou N, Meng D, Liang Z, Wang S. Salinity and nutrient condition as key factors drive the assembly of sediment prokaryotic communities. Int Biodeterior Biodegradation. 2024;193:105848. https://doi.org/10.1016/j.ibiod.2024.105848.
21. Zhao S, Banerjee S, White JF, Liu JJ, Zhou N, Tian CY. High salt stress increases archaeal abundance and network connectivity in saline agricultural soils. Catena (Amst). 2022;217. https://doi.org/10.1016/j.catena.2022.106520.
22. Wang H, Qi Z, Zheng P, Jiang C, Diao X. Abundant and rare microbiota assembly and driving factors between Mangrove and intertidal mudflats. Appl Soil Ecol. 2022;174. https://doi.org/10.1016/j.apsoil.2022.104438.
23. Bolyen E, Rideout JR, Dillon MR, Bokulich NA, Abnet CC, Al-Ghalith GA, et al. Reproducible, interactive, scalable and extensible Microbiome data science using QIIME 2. Nat Biotechnol. 2019;37:852–7.
24. Callahan BJ, McMurdie PJ, Rosen MJ, Han AW, Johnson AJA, Holmes SP. DADA2: High-resolution sample inference from illumina amplicon data. Nat Methods. 2016;13:581–3.
25. Yilmaz P, Parfrey LW, Yarza P, Gerken J, Pruesse E, Quast C, et al. The SILVA and All-species living tree project (LTP) taxonomic frameworks. Nucleic Acids Res. 2014;42:D643–8. https://doi.org/10.1093/nar/gkt1209.
26. Segata N, Izard J, Waldron L, Gevers D, Miropolsky L, Garrett WS, et al. Metagenomic biomarker discovery and explanation. Genome Biol. 2011;12:1–18.
27. Wemheuer F, Taylor JA, Daniel R, Johnston E, Meinicke P, Thomas T, et al. Tax4Fun2: prediction of habitat-specific functional profiles and functional

redundancy based on 16S rRNA gene sequences. Environ Microbiome. 2020;15:11. https://doi.org/10.1186/s40793-020-00358-7.
28. Csardi G, Nepusz T. The Igraph software package for complex network research. InterJournal complex systems 1695. Available at Igraph org/. Accessed November. 2006;30:2015.
29. Bastian M, Heymann S, Jacomy M. Gephi: an open source software for exploring and manipulating networks. Proc Int AAAI Conf Web Social Media. 2009;3:361–2. https://doi.org/10.1609/icwsm.v3i1.13937.
30. Brandes U. A faster algorithm for betweenness centrality. J Math Sociol. 2001;25:163–77.
31. Stegen JC, Lin X, Fredrickson JK, Chen X, Kennedy DW, Murray CJ, et al. Quantifying community assembly processes and identifying features that impose them. ISME J. 2013;7:2069–79. https://doi.org/10.1038/ismej.2013.93.
32. Van Den Wollenberg AL. Redundancy analysis an alternative for canonical correlation analysis. Psychometrika. 1977;42:207–19. https://doi.org/10.1007/BF02294050.
33. Ning D, Yuan M, Wu L, Zhang Y, Guo X, Zhou X, et al. A quantitative framework reveals ecological drivers of grassland microbial community assembly in response to warming. Nat Commun. 2020;11. https://doi.org/10.1038/s41467-020-18560-z.
34. Lin X, Hetharua B, Lin L, Xu H, Zheng T, He Z, et al. Mangrove sediment microbiome: adaptive microbial assemblages and their routed biogeochemical processes in Yunxiao Mangrove National nature Reserve, China. Microb Ecol. 2019;78:57–69. https://doi.org/10.1007/s00248-018-1261-6.
35. Wei P, Lei A, Zhou H, Hu Z, Wong Y, Tam NFY, et al. Comparison of microbial community structure and function in sediment between natural regenerated and original Mangrove forests in a National nature Mangrove Reserve, South China. Mar Pollut Bull. 2021;163. https://doi.org/10.1016/j.marpolbul.2020.111955.
36. Hartmann M, Brunner I, Hagedorn F, Bardgett RD, Stierli B, Herzog C, et al. A decade of irrigation transforms the soil Microbiome of a semi-arid pine forest. Mol Ecol. 2017;26:1190–206.
37. Naylor D, DeGraaf S, Purdom E, Coleman-Derr D. Drought and host selection influence bacterial community dynamics in the grass root Microbiome. ISME J. 2017;11:2691–704.
38. Naylor D, Coleman-Derr D. Drought stress and root-associated bacterial communities. Front Plant Sci. 2018;8:2223.
39. Preece C, Verbruggen E, Liu L, Weedon JT, Peñuelas J. Effects of past and current drought on the composition and diversity of soil microbial communities. Soil Biol Biochem. 2019;131:28–39.
40. Lareen A, Burton F, Schäfer P. Plant root-microbe communication in shaping root microbiomes. Plant Mol Biol. 2016;90:575–87.
41. Philippot L, Raaijmakers JM, Lemanceau P, Van Der Putten WH. Going back to the roots: the microbial ecology of the rhizosphere. Nat Rev Microbiol. 2013;11:789–99.
42. Bogino P, Abod A, Nievas F, Giordano W. Water-limiting conditions alter the structure and biofilm-forming ability of bacterial multispecies communities in the alfalfa rhizosphere. PLoS ONE. 2013;8:e79614.
43. Evans SE, Wallenstein MD. Soil microbial community response to drying and rewetting stress: does historical precipitation regime matter? Biogeochemistry. 2012;109:101–16.
44. Heděnec P, Singer D, Li J, Yao M, Lin Q, Li H, et al. Effect of dry-rewetting stress on response pattern of soil prokaryotic communities in alpine meadow soil. Appl Soil Ecol. 2018;126:98–106.
45. Lopez-Sangil L, Hartley IP, Rovira P, Casals P, Sayer EJ. Drying and rewetting conditions differentially affect the mineralization of fresh plant litter and extant soil organic matter. Soil Biol Biochem. 2018;124:81–9.
46. Lopes LD, Wang P, Futrell SL, Schachtman DP. Sugars and jasmonic acid concentration in root exudates affect maize rhizosphere bacterial communities. Appl Environ Microbiol. 2022;88:e00971–22.
47. Korenblum E, Massalha H, Aharoni A. Plant–microbe interactions in the rhizosphere via a circular metabolic economy. Plant Cell. 2022;34:3168–82.
48. Pantigoso HA, Newberger D, Vivanco JM. The rhizosphere microbiome: Plant–microbial interactions for resource acquisition. J Appl Microbiol. 2022;133:2864–76.
49. Bais HP, Weir TL, Perry LG, Gilroy S, Vivanco JM. The role of root exudates in rhizosphere interactions with plants and other organisms. Annu Rev Plant Biol. 2006;57:233–66.
50. Costa R, Götz M, Mrotzek N, Lottmann J, Berg G, Smalla K. Effects of site and plant species on rhizosphere community structure as revealed by molecular analysis of microbial guilds. FEMS Microbiol Ecol. 2006;56:236–49.
51. Wu P, Xiong X, Xu Z, Lu C, Cheng H, Lyu X, et al. Bacterial communities in the rhizospheres of three Mangrove tree species from Beilun Estuary, China. PLoS ONE. 2016;11. https://doi.org/10.1371/journal.pone.0164082.
52. Imchen M, Kumavath R, Barh D, Azevedo V, Ghosh P, Viana M, et al. Searching for signatures across microbial communities: metagenomic analysis of soil samples from Mangrove and other ecosystems. Sci Rep. 2017;7:8859. https://doi.org/10.1038/s41598-017-09254-6.
53. Andreote FD, Jiménez DJ, Chaves D, Dias ACF, Luvizotto DM, Dini-Andreote F, et al. The Microbiome of Brazilian Mangrove sediments as revealed by metagenomics. PLoS ONE. 2012;7:e38600.
54. Gong B, Cao H, Peng C, Perčulija V, Tong G, Fang H, et al. High-throughput sequencing and analysis of microbial communities in the Mangrove swamps along the Coast of Beibu Gulf in Guangxi, China. Sci Rep. 2019;9:9377.
55. Jamon-Haon E, Cuny P, Rossi A, Sylvi L, Fiard M, Militon C. Global biogeography of prokaryotes in Mangrove sediments: Spatial patterns and ecological insights from 16S rDNA metabarcoding. Estuar Coast Shelf Sci. 2025;325:109485. https://doi.org/10.1016/j.ecss.2025.109485.
56. Dyksma S, Bischof K, Fuchs BM, Hoffmann K, Meier D, Meyerdierks A, et al. Ubiquitous Gammaproteobacteria dominate dark carbon fixation in coastal sediments. ISME J. 2016;10:1939–53. https://doi.org/10.1038/ismej.2015.257.
57. Yan L, Kuang Y, Xie X, Peng K, Deng Y, Gan Y, et al. Insights into nitrogen biogeochemical cycling in Mangrove wetland from Genome-Resolved metagenomic sequencing. J Hydrol (Amst). 2024;640. https://doi.org/10.1016/j.jhydrol.2024.131741.
58. Muyzer G, Stams AJM. The ecology and biotechnology of sulphate-reducing bacteria. Nat Rev Microbiol. 2008;6:441–54.
59. Schauder R, Widdel F, Fuchs G. Carbon assimilation pathways in sulfate-reducing bacteria II. Enzymes of a reductive citric acid cycle in the autotrophic Desulfobacter hydrogenophilus. Arch Microbiol. 1987;148:218–25.
60. Durbin KJ, Watanabe I. Sulfate-reducing bacteria and nitrogen fixation in flooded rice soil. Soil Biol Biochem. 1980;12:11–4.
61. Shih PM, Ward LM, Fischer WW. Evolution of the 3-hydroxypropionate bicycle and recent transfer of anoxygenic photosynthesis into the Chloroflexi. Proc Natl Acad Sci. 2017;114:10749–54.
62. Sylvia H, Andreas B, Georg F, l-Malyl-Coenzyme A. Lyase/β-Methylmalyl-Coenzyme A lyase from Chloroflexus aurantiacus, a bifunctional enzyme involved in autotrophic CO2 fixation. J Bacteriol. 2002;184:5999–6006. https://doi.org/10.1128/jb.184.21.5999-6006.2002.
63. Potter C, Freeman C, Golyshin PN, Ackermann G, Fenner N, McDonald JE, et al. Subtle shifts in microbial communities occur alongside the release of carbon induced by drought and rewetting in contrasting peatland ecosystems. Sci Rep. 2017;7:11314.
64. Bouskill NJ, Wood TE, Baran R, Ye Z, Bowen BP, Lim H, et al. Belowground response to drought in a tropical forest soil. I. Changes in microbial functional potential and metabolism. Front Microbiol. 2016;7:525.
65. Bouskill NJ, Lim HC, Borglin S, Salve R, Wood TE, Silver WL, et al. Pre-exposure to drought increases the resistance of tropical forest soil bacterial communities to extended drought. ISME J. 2013;7:384–94.
66. Aleklett K, Leff JW, Fierer N, Hart M. Wild plant species growing closely connected in a subalpine meadow host distinct root-associated bacterial communities. PeerJ. 2015;3:e804.
67. Cram JA, Xia LC, Needham DM, Sachdeva R, Sun F, Fuhrman JA. Cross-depth analysis of marine bacterial networks suggests downward propagation of Temporal changes. ISME J. 2015;9:2573–86. https://doi.org/10.1038/ismej.2015.76.
68. Jiang Y, Sun B, Li H, Liu M, Chen L, Zhou S. Aggregate-related changes in network patterns of nematodes and ammonia oxidizers in an acidic soil. Soil Biol Biochem. 2015;88:101–9. https://doi.org/10.1016/j.soilbio.2015.05.013.
69. Faust K, Raes J. Microbial interactions: from networks to models. Nat Rev Microbiol. 2012;10:538–50. https://doi.org/10.1038/nrmicro2832.
70. Röttjers L, Faust K. From hairballs to hypotheses–biological insights from microbial networks. FEMS Microbiol Rev. 2018;42:761–80. https://doi.org/10.1093/femsre/fuy030.
71. May RM. Will a large complex system be stable? Nature. 1972;238:413–4. https://doi.org/10.1038/238413a0
72. Vallina SM, Le Quéré C. Stability of complex food webs: Resilience, resistance and the average interaction strength. J Theor Biol. 2011;272:160–73. https://doi.org/10.1016/j.jtbi.2010.11.043.
73. Ratzke C, Barrere J, Gore J. Strength of species interactions determines biodiversity and stability in microbial communities. Nat Ecol Evol. 2020;4:376–83. https://doi.org/10.1038/s41559-020-1099-4.

Publisher's Note